A SAMPLING-BASED APPROACH TO SPACECRAFT AUTONOMOUS MANEUVERING WITH SAFETY SPECIFICATIONS

Joseph A. Starek[*], Brent Barbee[†], and Marco Pavone[‡]

This paper presents a method for *safe* spacecraft autonomous maneuvering that leverages robotic motion planning techniques to spacecraft control. Specifically, the scenario we consider is an in-plane rendezvous of a chaser spacecraft in proximity to a target spacecraft at the origin of the Clohessy-Wiltshire-Hill frame. The trajectory for the chaser spacecraft is generated in a receding-horizon fashion by executing a sampling-based robotic motion planning algorithm named Fast Marching Trees (FMT[*]), which efficiently grows a tree of trajectories over a set of probabilistically-drawn samples in the state space. To enforce safety, the tree is only grown over *actively safe samples,* from which there exists a one-burn collision avoidance maneuver that circularizes the spacecraft orbit along a collision-free coasting arc and that can be executed under potential thruster failures. The overall approach establishes a provably-correct framework for the *systematic* encoding of safety specifications into the spacecraft trajectory generation process and appears promising for *real-time* implementation on orbit. Simulation results are presented for a two-fault tolerant spacecraft during autonomous approach to a single client in Low Earth Orbit.

INTRODUCTION

Autonomous execution of spacecraft proximity operations requires the real-time computation of spacecraft trajectories that must satisfy collision avoidance, plume impingement [1, 2], sensor field-of-view, and a number of other complex navigation constraints [3, Ch. 4]. To make matters worse, the trajectory generation process is complicated by the need to meet stringent safety specifications in the face of a wide variety and number of failure modes [4]. The objective of this paper is to devise a computationally-efficient method for enforcing infinite-horizon hard collision safety specifications for autonomous spacecraft proximity operations in the face of probabilistic control failures. Specifically, this work embeds the rendezvous trajectory design problem for an impulsive spacecraft within the context of safety-constrained robotic motion planning [5] in order to robustify the planning process to thruster stuck-off failures and facilitate real-time autonomous escape trajectory generation on orbit. Due to the fuel-limited nature of many spacecraft missions, emphasis is placed on finding minimum-Δv escape maneuvers in order to improve mission reattempt opportunities. Along these lines, we prioritize the use of *active safety* measures (which allow actuated Collision Avoidance Maneuvers or CAMs) over passive safety guarantees (which shut off all thrusters and restrict the system to zero control, thereby conservatively limiting the search space of possible escape maneuvers to coasting arcs).

Our approach extends earlier sampling-based treatments of spacecraft autonomous maneuvering [5–7] through the use of actuated escape maneuvers with trajectory safety constraints defined by positively-invariant sets, similar, *e.g*., to [8–12]. Our key contributions are the deterministic guarantee of safe transfers up to a given thruster fault tolerance under potential stuck-off failures, the use continuous full-state dynamics (including attitude), and the ability to use arbitrary state-space samples. Our work automates (roughly-speaking) the safety-constrained rendezvous design process taken by Barbee et al. [13].

[*]Graduate Student, Dept. of Aeronautics & Astronautics, Stanford University, Durand Building, 496 Lomita Mall, Rm 009, Stanford, CA, 94305-4035, USA

[†]Aerospace Engineer, Navigation and Mission Design Branch (Code 595), NASA Goddard Space Flight Center, 8800 Greenbelt Rd, Bldg 11, C002H, Greenbelt, MD, 20771-2400, USA

[‡]Assistant Professor, Dept. of Aeronautics & Astronautics, Stanford University, Durand Building, 496 Lomita Mall, Rm 261, Stanford, CA, 94305-4035, USA

The structure of the paper is as follows. We begin by formalizing the definition of infinite-time vehicle safety under control errors, then reformulate it as a finite-horizon mathematical optimization problem using the notion of safe, stable positively-invariant sets. The problem is designed to certify the safety of a particular vehicle state using the standard sampling and collision-checking routines of sampling-based robotic motion planning algorithms. If enforced for all samples, safety of the resulting motion planning solution is assured. This framework is then specialized to spacecraft maneuvering in Low Earth Orbit (LEO), from which our active safety strategy is motivated and derived. Numerical simulations using Fast Marching Trees (FMT*) then follow, illustrating the method's effectiveness and improvement over safety-unconstrained planning.

VEHICLE SAFETY

Consistent with the notions proposed by Schouwenaars et al. [14], Wehse [3, 4.1.2], and Fraichard [15], the definition of vehicle safety in this paper is taken as the following:

Definition 1 (Vehicle Safety). A vehicle state is considered *safe* if and only if there exists, under the worst-possible environment and failure conditions, a collision-free, dynamically-feasible trajectory satisfying the constraints that navigates the vehicle to a sequence of states in which it can remain indefinitely.

Note *indefinitely** is a critical component of the definition. Trajectories without infinite-horizon safety guarantees can ultimately violate constraints [11] and are therefore a potential risky choice that can defeat the purpose of using a hard constraint in the first place. Hence throughout this work we will impose safety constraints over an infinite-horizon (or, as we will show using invariant sets, an *effectively* infinite horizon).

Consider now a vehicle system with state vector $\mathbf{x} \in \mathcal{X}$ and control vector $\mathbf{u} \in \mathcal{U}(\mathbf{x})$ that evolves over time $t \in \mathcal{T} = [t_0, \infty)$ according to dynamics $\dot{\mathbf{x}} = f(\mathbf{x}, \mathbf{u}, t)$. Let $\mathcal{T}_{\text{fail}} \subseteq \mathcal{T}$ represent the set of possible failure times (for instance, a set of prescribed burn times $\{\tau_i\}$, the final approach phase $\mathcal{T}_{\text{approach}}$, or the entire maneuver duration $\mathcal{T}$). When a failure occurs, control authority is lost through a reduction in actuator functionality, negatively impacting system controllability. Let $\mathcal{U}_{\text{fail}}(\mathbf{x}) \subset \mathcal{U}(\mathbf{x})$ represent the new control set, where we assume that $\mathbf{0} \in \mathcal{U}_{\text{fail}}$ for all $\mathbf{x}$ (i.e. we assume that no actuation is always a feasible option). Mission safety is commonly imposed in two different ways [3, 4.4]:

- *Passive Safety*: For all possible $t_{\text{fail}} \in \mathcal{T}_{\text{fail}}$, ensure that $\mathbf{x}(t_{\text{fail}})$ satisfies Definition 1 with $\mathbf{u}(t) = \mathbf{0}$ for all $t \geq t_{\text{fail}}$. For spacecraft, this means its coasting arc from the point of failure must be safe for all time (though practically this is imposed only over a finite horizon).

- *Active Safety*: For all possible $t_{\text{fail}} \in \mathcal{T}_{\text{fail}}$ and failure modes $\mathcal{U}_{\text{fail}}$, design actuated collision avoidance maneuvers to satisfy Definition 1 with $\mathbf{u}(t) \in \mathcal{U}_{\text{fail}}$ for all $t \geq t_{\text{fail}}$, where $\mathbf{u}(t)$ is not necessarily restricted to $\mathbf{0}$.

In much of the literature, only passive safety is considered out of a need for tractability (to avoid verification over a combinatoric explosion of failure mode possibilities) and in order to capture the common failure mode in which control authority is lost completely. Though considerably simpler to implement, this approach potentially neglects many mission-saving control policies.

Maneuver to a safe, stable, positively-invariant set

Instead of evaluating trajectory safety for all future times $t \geq t_{\text{fail}}$, it is generally more practical to consider finite-time solutions starting at $\mathbf{x}(t_{\text{fail}})$ that terminate at a point inside a safe positively invariant set $\mathcal{X}_{\text{invariant}}$. If the maneuver is safe and the invariant set is safe for all time, then safety of the vehicle is assured.

Definition 2 (Positively Invariant Set). A set $\mathcal{M}$ is positively invariant with respect to $\dot{\mathbf{x}} = f(\mathbf{x})$ if and only if $\mathbf{x}(0) \in \mathcal{M} \Rightarrow \mathbf{x}(t) \in \mathcal{M}, t \in \mathbb{R}_+$.

This yields the following problem for finite-time verification of trajectory safety:

---

*"Indefinite" here implies sufficiently-long for all practical purposes under the accuracy of the dynamics model.

Definition 3 (Finite-Time Trajectory Safety Verification). For all $t_{\text{fail}} \in \mathcal{T}_{\text{fail}}$ and for all $\mathcal{U}_{\text{fail}}(\mathbf{x}(t_{\text{fail}})) \subset \mathcal{U}(\mathbf{x}(t_{\text{fail}}))$, there exists $\{\mathbf{u}(\tau), \tau \geq t_{\text{fail}}\} \in \mathcal{U}_{\text{fail}}(\mathbf{x}(t_{\text{fail}}))$ and $T > t_{\text{fail}}$ such that $\mathbf{x}(\tau) \in \mathcal{X}_{\text{free}}, t_{\text{fail}} \leq \tau \leq T$ and $\mathbf{x}(T) \in \mathcal{X}_{\text{invariant}} \subseteq \mathcal{X}_{\text{free}}$.

where T is some finite safety verification horizon time. Though in principle any *safe* positively-invariant set $\mathcal{X}_{\text{invariant}}$ is acceptable, not just any will do in practice; in real-world scenarios, unstable trajectories caused by model uncertainties could cause state divergence towards configurations whose safety has not been verified. Hence care must be taken to use only *stable* positively-invariant sets*.

Combining Definition 3 with other control constraints and slightly adjusting the notation, vehicle safety verification after a failure at $\mathbf{x}_0$ can be expressed in its full generality as the following optimization problem in decision variables $t_{\text{f}} \in [t_0, \infty)$, $\mathbf{x}(t) \in \mathbb{R}^N$, and $\mathbf{u}(t) \in \mathbb{R}^M$, for $t \in [t_0, t_{\text{f}}]$:

$$\underset{t_{\text{f}},\mathbf{x}(t),\mathbf{u}(t)\in\mathcal{U}_{\text{fail}}(\mathbf{x}_0)}{\text{minimize}} \quad J(\mathbf{x}(t), \mathbf{u}(t), t) \tag{1}$$

$$\begin{aligned}
\text{subject to} \quad & \dot{\mathbf{x}}(t) = f(\mathbf{x}(t), \mathbf{u}(t), t) && \text{(Dynamics)} \\
& \mathbf{x}(t_0) = \mathbf{x}_0 && \text{(Initial Condition)} \\
& \mathbf{x}(t_{\text{f}}) \in \mathcal{X}_{\text{invariant}} && \text{(Invariant Set Termination)} \\
& g_i(\mathbf{x}, \mathbf{u}) \leq 0, \quad i = [1, \dots, p] && \text{(Inequality Constraints)} \\
& h_j(\mathbf{x}, \mathbf{u}) = 0, \quad j = [1, \dots, q] && \text{(Equality Constraints)}
\end{aligned}$$

where here g_i and h_j represent the inequality and equality constraints, respectively, imposed for ensuring escape maneuver safety (*e.g.*, to avoid a collision), and $\mathcal{X}_{\text{invariant}}$ denotes the space of safe, invariant state trajectories. Typically we seek any feasible solution following a failure, in which case we can take $J = 1$.

Fault-Tolerant Safety Strategy

The difficulty of solving the finite-time trajectory safety problem lies in the fact that a feasible solution must be found for *all* possible failure times (typically assumed to be any time during the mission) as well as for *all* possible failures. To illustrate, for a K-fault tolerant spacecraft with N control components (thrusters, momentum wheels, CMG's, etc) that we each model as either "operational" and "failed," this yields a total of:

$$N_{\text{fail}} = \sum_{k=0}^{K} \binom{N}{k} = \sum_{k=0}^{K} \frac{N!}{(N-k)!k!}$$

possible optimization problems that must be solved for every time t_{fail} along the design trajectory†. By any standard, this is intractable, and hence explains why so often *passive* safety guarantees are selected (requiring only one control configuration check instead of N_{fail}, since we prescribe $\mathbf{u} = \mathbf{0}$ which we know lies in $\mathcal{U}_{\text{fail}}$ given our assumption. This is analogous to setting $k = N$ with $K \triangleq N$). One idea for simplifying the problem while still satisfying safety (Equation (1)), which we employ here, consists of the following strategy:

Theorem 4 (Fault-Tolerant Active Safety). *To solve Equation* (1)*, it is sufficient (but not necessary) to implement the following procedure:*

1. *From each $\mathbf{x}(t_{fail})$, prescribe a Collision-Avoidance Maneuver (CAM) Π_{CAM} (that is, an escape policy) that gives a horizon time T and escape control sequence $\mathbf{u} = \Pi_{CAM}(\mathbf{x})$ designed to automatically satisfy $\mathbf{u}(\tau) \subset \mathcal{U}$ for all $t_{fail} \leq \tau \leq T$ and $\mathbf{x}(T) \in \mathcal{X}_{invariant}$.*

2. *For each possible failure mode $\mathcal{U}_{fail}(\mathbf{x}(t_{fail})) \subset \mathcal{U}(\mathbf{x}(t_{fail}))$ up to tolerance K, determine if the control law is feasible; that is, see if $\mathbf{u} = \Pi_{CAM}(\mathbf{x}) \subset \mathcal{U}_{fail}$ for the particular failure in question.*

---

*One way to determine and assess the stability of these positively-invariant sets is the well-known LaSalle Invariant Set Theorem [16]

†Each spacecraft configuration under k possible failures of N control components can be modeled as choosing k components out of N for failure, which we sum up to tolerance K.

This effectively removes decision variables **u** from Equation (1), allowing simple numerical integration for satisfaction of the dynamic constraints, an *a posteriori* verification of the control constraints g_i and h_j, and a final test of control feasibility (a simple LP for spacecraft with body-fixed actuators). This checks if the given CAM, guaranteed to provide a safe escape route, can actually be accomplished in the given failure situation. The approach is conservative due to the fact that the control is imposed and not derived; however, the advantage is a greatly simplified optimal control problem with difficult-to-handle constraints relegated to a posteriori checks. Note that formal definitions of safety require that this be satisfied for all possible failure modes of the spacecraft — we do not avoid the combinatoric explosion of N_{fail}. However, the feasibility problems are each greatly simplified — reduced to control allocation LP's for the case of impulsively-actuated spacecraft – and with K typically restricted to at most 3, the problem remains tractable. The difficult part, then, lies in computing Π_{CAM}, but this can easily be derived in an off-line fashion. Hence, the strategy should work well for vehicles with difficult, non-convex objective functions and constraints, and particularly well in cases where the problem can be convexified by removing the control vector **u** from the decision variables.

SAFETY IN CWH DYNAMICS

We now apply the ideas of the previous section to the specific case of an in-plane rendezvous of a servicing spacecraft (or "chaser") in proximity to a target spacecraft (or "client") in circular orbit at the origin of the Clohessy-Wiltshire-Hill (CWH) Local-Vertical, Local-Horizontal (LVLH) frame. When resolved in this rotating reference frame, the chaser dynamics linearized about the target orbit have been shown to obey the following unforced state-transition equations [17]. Let $\theta = n(t - t_0)$ be the true anomaly/polar angle of the client relative to an inertial axis in its orbital plane, where n is the client mean motion. As shown in Figure 1, let δx, δy, and δz be the cross-track (radial), in-track (circumferential) and out-of-plane positions of the chaser relative to the client, and let $\delta\dot{x}$, $\delta\dot{y}$, and $\delta\dot{z}$ be its corresponding velocities. Then:

$$\delta x = (4 - 3\cos\theta)\delta x_0 + \left(\frac{1}{n}\sin\theta\right)\delta\dot{x}_0 + \left(\frac{2}{n}(1 - \cos\theta)\right)\delta\dot{y}_0 \tag{2a}$$

$$\delta y = (6\sin\theta - 6\theta)\delta x_0 + \left(\frac{2}{n}(\cos\theta - 1)\right)\delta\dot{x}_0 + \delta y_0 + \left(\frac{1}{n}(4\sin\theta - 3\theta)\right)\delta\dot{y}_0 \tag{2b}$$

$$\delta z = (\cos\theta)\delta z_0 + \left(\frac{1}{n}\sin\theta\right)\delta\dot{z}_0 \tag{2c}$$

$$\delta\dot{x} = (3n\sin\theta)\delta x_0 + (\cos\theta)\delta\dot{x}_0 + (2\sin\theta)\delta\dot{y}_0 \tag{2d}$$

$$\delta\dot{y} = (6n(\cos\theta - 1))\delta x_0 + (-2\sin\theta)\delta\dot{x}_0 + (4\cos\theta - 3)\delta\dot{y}_0 \tag{2e}$$

$$\delta\dot{z} = (-n\sin\theta)\delta z_0 + (\cos\theta)\delta\dot{z}_0 \tag{2f}$$

A "Keep-Out Zone" (KOZ), typically ellipsoidal and denoted as $\mathcal{X}_{\text{KOZ}}$, is defined about the target in the CWH frame. Throughout its approach, the chaser must certify that it will not enter this KOZ up to a thruster fault tolerance. Per Definition 3, this necessitates a search for a safe invariant set for finite-time escape along with, as outlined by Theorem 4, the definition of an escape policy Π_{CAM}, which we describe next.

CAM Policy

For mission safety following a failure under CWH dynamics, Definition 3 requires us to find a terminal state in an invariant set $\mathcal{X}_{\text{invariant}}$ entirely contained within the free state space $\mathcal{X}_{\text{free}}$. We choose for $\mathcal{X}_{\text{invariant}}$ the set of circularized orbits that skip the radial band spanned by the KOZ ellipse. The reason this is necessary is that any attempts to circularize within this band would result in an eventual collision with the target KOZ, either in the short-term or after nearly one full synodic period. In the event of an unrecoverable failure or abort scenario requiring longer than one synodic period to resolve from the ground, circularization here would jeopardize the target and fail to satisfy Definition 1. Such a band is called a zero-thrust "Region of Inevitable Collision (RIC)," as without intervention a collision with the KOZ is imminent and certain. Fortunately, the zero-thrust RIC, which we denote as $\mathcal{X}_{\text{ric}}$, can be identified by inspection in this case; its complement, therefore, is a safe invariant set $\mathcal{X}_{\text{invariant}}$ that we can use to terminate safe escape maneuvers. As a result, for the coplanar
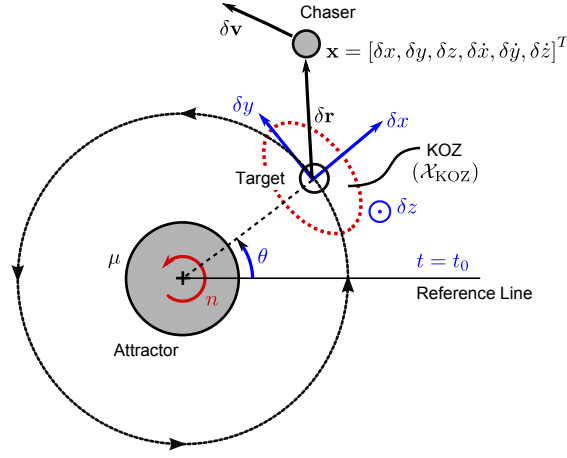
Figure 1. Illustration of the CWH targeting scenario and Keep-Out Zone (KOZ). n is the mean motion of the target spacecraft orbit, θ is its mean anomaly, t denotes time, $\delta\mathbf{r}$ and $\delta\mathbf{v}$ the chaser relative position and velocity, and $(\delta x, \delta y, \delta z)$ **LVLH coordinates.** The frame rotates with the target as it orbits the gravitational attractor, μ.

case, *any CAM policy that circularizes the chaser orbit at a position outside of this radial band would be guaranteed safe.* See Equations (3)–(5) for a mathematical description, and Figure 2 for an illustration.

$$\mathcal{X}_{\text{KOZ}} = \left\{\mathbf{x} \mid \mathbf{x}^{\mathrm{T}}\mathbf{R}\mathbf{x} \geq 1, \text{ where } \mathbf{R} = \operatorname{diag}\left(\rho_{\delta x}^{-2}, \rho_{\delta y}^{-2}, \rho_{\delta z}^{-2}, 0, 0, 0\right), \text{ with } \rho_i \text{ representing} \right. \tag{3}$$

the ellipsoidal KOZ semi-axis in the i-th LVLH frame axis direction.$\}$

$$\mathcal{X}_{\text{ric}} = \left\{\mathbf{x} \mid |\delta x| < \rho_{\delta x}, \delta\dot{x} = 0, \delta\dot{y} = -\frac{3}{2}n\delta x\right\} \supset \mathcal{X}_{\text{KOZ}} \tag{4}$$

$$\mathcal{X}_{\text{invariant}} = \left\{\mathbf{x} \mid |\delta x| \geq \rho_{\delta x}, \delta\dot{x} = 0, \delta\dot{y} = -\frac{3}{2}n\delta x\right\} = \mathcal{X}_{\text{ric}}^{\mathsf{c}} \tag{5}$$
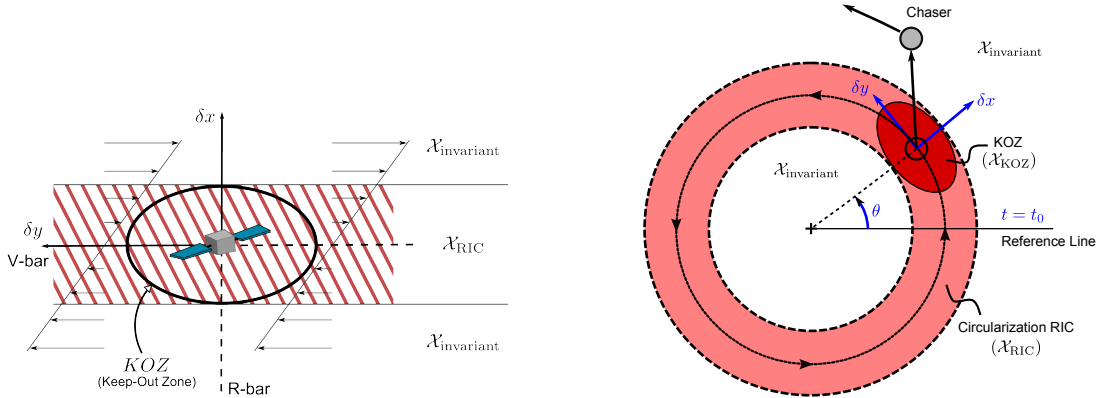
(a) Safe circularization burn zones $\mathcal{X}_{\text{invariant}}$ for planar CWH dynamics. Any circularization attempts inside $\mathcal{X}_{\text{ric}}$ will result in eventual penetration of the client KOZ, as indicated by the arrows.

(b) Inertial view of the radial band spanned by the KOZ that defines the RIC. Its complement shows the invariant positions in $\mathcal{X}_{\text{invariant}}$ used for safe trajectory escape maneuver targeting.

Figure 2. Visualizing the Safe and Unsafe Circularization Regions Used by the CAM Safety Policy

In short, our CAM policy to safely escape from a state $\mathbf{x}$ at which the spacecraft arrives (possibly under

5

failures) at time t consists of the following:

1. Coast from $\mathbf{x}(t)$ to some new $T > t$ such that $\mathbf{x}(T^-)$ lies at a position in $\mathcal{X}_{\text{invariant}}$.

2. Circularize the orbit at $\mathbf{x}(T)$ such that $\mathbf{x}(T^+) \in \mathcal{X}_{\text{invariant}}$.

3. Coast along the new orbit (horizontal drift along the in-track axis in the CWH relative frame) in $\mathcal{X}_{\text{invariant}}$ until allowed to continue the mission (*e.g.*, after approval from ground operators).

Determining the Circularization Time, T

In the event of a thruster failure at state $\mathbf{x}(t)$ that requires an emergency CAM, the time $T > t$ at which to attempt a circularization maneuver after coasting from $\mathbf{x}(t)$ becomes a degree of freedom. As we intend to maximize the recovery chances of the chaser spacecraft in the event of a failure, we choose T so as to minimize the cost of the circularization burn $\mathbf{\Delta v}_{\text{circ}}$, whose magnitude we denote Δv_{circ}. Details on the approach, heavily optimized for speed, have been relegated to Appendix A.

Verifying CAM Policy Feasibility

Once the circularization burn time is determined, feasibility of the escape trajectory under the failure configuration at $\mathbf{x}(t)$ is all that remains to determine whether the chaser spacecraft can execute it. It can be shown that, when attempting to solve the minimum-control-effort allocation problem for rigid-body spacecraft (in this case, the minimum-Δv allocation problem), thruster magnitudes can be obtained by solving a simple LP [18], typically accomplished on the order of milliseconds.

Actively-Safe CWH Targeting

Combining these tools together, CWH targeting with built-in actively-safe CAM trajectories can be represented collectively as Algorithms 1–2. The approach is presented in the form of two subroutines: SAMPLEFREE and COLLISIONFREE, standard functions within the sampling-based motion planning paradigm. Sampling-based planning [5, 19, 20] essentially breaks down a global continuous trajectory optimization problem into a series of smaller, simpler optimal control problems through intelligent sampling and expansion towards intermediate waypoints in the collision-free configuration space $\mathcal{X}_{\text{free}}$. SAMPLEFREE implements a sampling scheme in which we save only those states in the configuration space $\mathcal{X}$ for which we can find escape policies as described previously. COLLISIONFREE tests whether a steering trajectory formulated between two sampled states $\mathbf{x}_i$ and $\mathbf{x}_f$ meets mission constraints, avoids the target KOZ, and satisfies the control allocation problem for both the nominal path as well as all CAMs under all potential failure conditions.

Algorithm 1 Samples the free configuration space. Ensures that only actively-safe sample points are available for expansion during execution of the FMT* algorithm.

1: **function** SAMPLEFREE($\mathcal{X}$, N_{samples}, t_0)
2:     Initialize $\mathcal{S}$ as $\mathcal{S} \leftarrow \varnothing$
3:     **while** $\mathcal{S}$ has less than N_{samples} samples
4:         Sample a new state as $\mathbf{s} \leftarrow$ SAMPLE($\mathcal{X}$)
5:         Implement the CAM policy from $\mathbf{s}$ as $[\mathbf{u}_{\text{CAM}}, T] \leftarrow \Pi_{\text{CAM}}(\mathbf{s}(t_0))$
6:         Compute the CAM trajectory $\mathbf{x}_{\text{CAM}}(t_{\text{CAM}}) = \int_{t_0}^{T} f(\mathbf{x}, \mathbf{u}_{\text{CAM}}, \tau)\, \mathrm{d}\tau$
7:         **if** COLLISIONFREE($\mathbf{x}_{\text{CAM}}, \mathbf{u}_{\text{CAM}}, t_{\text{CAM}}$)
8:             Add $\mathbf{s}$ to $\mathcal{S}$
9:     **return** $\mathcal{S}$

Combined with the steering algorithm described in Appendix B, this yields a generalized formulation for actively-safe CWH targeting that can be implemented using any asymptotically-optimal sampling-based motion planner (though our algorithm of choice will be the Fast Marching Trees (FMT*) algorithm [21], represented in pseudocode as Algorithm 3). FMT* intelligently expands a tree of feasible paths from an initial state $\mathbf{x}_{\text{init}}$ to a goal state $\mathbf{x}_{\text{goal}}$ around obstacles. As it makes connections, it relies on adding and

Algorithm 2 Tests if the trajectory $\mathbf{x}(t)$ generated under control $\mathbf{u}(t)$ (namely, a series of impulses $\mathbf{\Delta v}(\tau)$ applied at times $\tau = [\tau_1, \ldots, \tau_N]$) meets mission constraints (particularly CAM safety constraints).

1: **function** COLLISIONFREE($\mathbf{x}(t), \mathbf{u}(t), t$)
2:     safe = (**all** $t \leq T_{\max}$) **and** (**all** $\mathbf{x} \in \mathcal{X}$) **and** (**all** $\mathbf{x} \notin \mathcal{X}_{\mathrm{KOZ}}$)
3:     If safe, start with burn $k = 1$
4:     **while** safe **and** $k \leq N$
5:         Test the feasibility of nominal burn $\mathbf{\Delta v}(\tau_k)$ (impingement/control feasibility)
6:         **for each** failure $f \in \mathcal{U}_{\mathrm{fail}}(\mathbf{x}(\tau_k))$ (including no failure)
7:             Test the feasibility of CAM burn $\mathbf{\Delta v}_{\mathrm{CAM}}(T_k)$ under failure f (**break** if infeasible)
8:         safe = **false** if nominally infeasible or a CAM is infeasible under any failure
9:         $k = k + 1$
10:    **return** safe

---

removing nodes (waypoint states) from three sets: a set of unexplored nodes $\mathcal{V}_{\mathrm{unvisited}}$ not yet connected by the algorithm, a frontier $\mathcal{V}_{\mathrm{open}}$ of nodes likely to make efficient connections to unexplored neighbors, and an interior $\mathcal{V}_{\mathrm{closed}}$ of nodes that are no longer useful for exploring the state space $\mathcal{X}$. Refer to [21] for full details.

When called to solve for a path from $\mathbf{x}_{\mathrm{init}}$ to $\mathbf{x}_{\mathrm{goal}}$ using N_{samples} free-space sample points, this approach is *guaranteed* (by our careful construction) to return a trajectory, if one exists, that minimizes the Δv cost of connecting the two states through the given set of N_{samples} sample points subject to the mission constraints and for which there exists a safe and available CAM trajectory from each state along the path under all failures f considered in $\mathcal{U}_{\mathrm{fail}}$. As we show, this can be used to guarantee the availability of escape trajectories during CWH proximity operations under a maximum control fault-tolerance.

Algorithm 3 The Fast Marching Tree Algorithm (FMT*). Computes a minimal-cost path from a given initial state $\mathbf{x}(t_0) = \mathbf{x}_{\mathrm{init}}$ to a target state $\mathbf{x}_{\mathrm{goal}}$, through a fixed number N_{samples} of samples $\mathcal{S}$. When SAMPLEFREE and/or COLLISIONFREE account for safety constraints, FMT* can generate actively-safe paths.


1: Add $\mathbf{x}_{\mathrm{init}}$ to the root of the tree $\mathcal{T}$, as a member of the frontier set $\mathcal{V}_{\mathrm{open}}$
2: Generate samples $\mathcal{S} \leftarrow$ SAMPLEFREE($\mathcal{X}, N_{\mathrm{samples}}, t_0$) and add them to the unexplored set $\mathcal{V}_{\mathrm{unvisited}}$
3: Set the lowest-cost node in the tree as $\mathbf{z} \leftarrow \mathbf{x}_{\mathrm{init}}$
4: **while true**
5:     **for** each neighbor $\mathbf{x}$ of $\mathbf{z}$ in $\mathcal{V}_{\mathrm{unvisited}}$
6:         Find the neighbor $\mathbf{x}_{\min}$ in $\mathcal{V}_{\mathrm{open}}$ of cheapest cost-to-go to $\mathbf{x}$
7:         Compute the trajectory between them as $[\mathbf{x}(t), \mathbf{u}(t), t] \leftarrow$ STEER($\mathbf{x}_{\min}, \mathbf{x}$) (*see Appendix B*)
8:         **if** COLLISIONFREE($\mathbf{x}(t), \mathbf{u}(t), t$)
9:             Add the trajectory from $\mathbf{x}_{\min}$ to $\mathbf{x}$ to the tree $\mathcal{T}$
10:    Add successful $\mathbf{x}$ to $\mathcal{V}_{\mathrm{open}}$ and remove them from the unexplored set $\mathcal{V}_{\mathrm{unvisited}}$
11:    Remove $\mathbf{z}$ from the frontier $\mathcal{V}_{\mathrm{open}}$ and add it to $\mathcal{V}_{\mathrm{closed}}$
12:
13:    **if** $\mathcal{V}_{\mathrm{open}}$ is empty
14:        **return** Failure
15:    Reassign $\mathbf{z}$ as the node in $\mathcal{V}_{\mathrm{open}}$ with smallest cost-to-come from the root ($\mathbf{x}_{\mathrm{init}}$)
16:    **if** $\mathbf{z}$ is in the goal region $\mathcal{X}_{\mathrm{goal}}$
17:        **return** Success, and the unique path from the root ($\mathbf{x}_{\mathrm{init}}$) to $\mathbf{z}$


SIMULATIONS

The scenario considered in this paper is modeled as the approach phase of a satellite servicing mission, in which a servicer spacecraft seeks to rendezvous and dock with an uncooperative client moving in a well-defined, circular orbit in LEO. We use the Landsat-7 mission as a reference [22, 3.2] (see Figure 3(a)–(b)), in line with current robotic servicing studies at NASA.
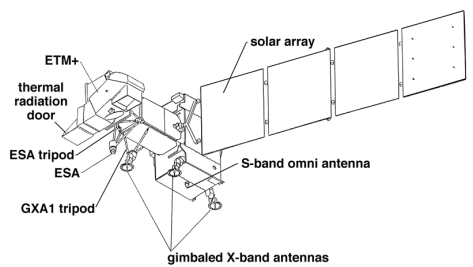
(a) Landsat-7 Schematic (Nadir (-δx direction) is oriented downwards, while the in-track ($+\delta y$) direction is pointing leftwards).
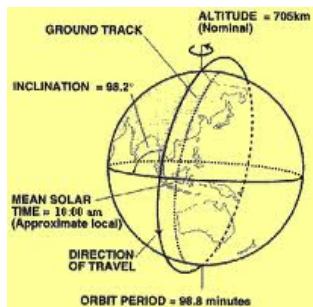
(b) Landsat-7 Orbit (Image courtesy of the Landsat-7 Science Data Users Handbook).
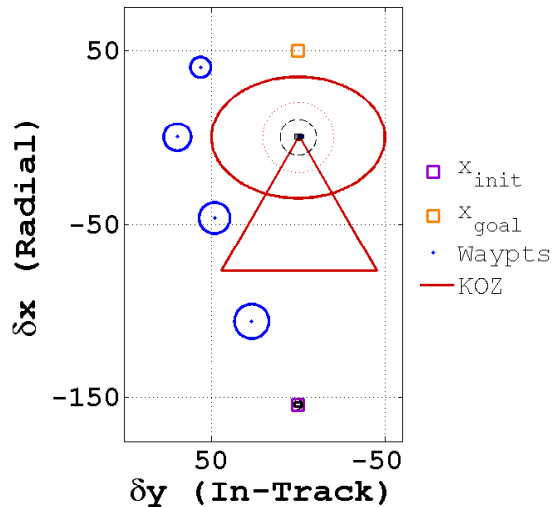
(c) Motion planning query used for numerical experiments. The spacecraft must track a series of guidance waypoints to the goal, located radially above the client. Positional goal tolerances are visualized as circles around each waypoint, which successively shrink in size.

Figure 3. Target Spacecraft and Orbit Scenario Used for Numerical Experiments

Setup

The rendezvous maneuver is assumed to begin sufficiently close to the target* after insertion into a lower coplanar circular orbit. We imagine the chaser must be repositioned for a near-field approach from above. Let $\mathbf{x} = [\delta x, \delta y, \delta z, \delta \dot{x}, \delta \dot{y}, \delta \dot{z}]^T$ represent the position and velocity, respectively, of the chaser center-of-mass relative to the target center-of-mass resolved in the Clohessy-Wiltshire-Hill (CWH) Local-Vertical, Local-Horizontal (LVLH) frame. From its initial state, the chaser is required to navigate to a sequence of pre-specified CWH position waypoints, eventually terminating at a fixed goal position. For nominal maneuvering, an attitude controller is assumed to stabilize the chaser in a nadir-pointing attitude. Should a CAM become necessary, the chaser is assumed to initiate the smallest possible "turn and burn" slew maneuver to reorient a remaining thruster for the CAM circularization burn (such that CAM thruster allocation is always possible with at least one working thruster, given enough time for the slew). Details are omitted here due to space limitations. Throughout the maneuver, the chaser must avoid entering the elliptic target KOZ, enforce hard safety constraints with regard to a two-fault tolerance to stuck-off thruster failures [3, 4.1.1], and otherwise avoid interfering with the target (including avoiding LandSat-7's nadir-pointing communication lobes (represented by a truncated half-cone), or impinging its surfaces with exhaust).

The FMT* planning algorithm [21] is called once for each waypoint in the guidance sequence, and their solutions linked to yield an overall solution to the planning problem. Each subsequent call programmatically defines new axes-aligned configuration search spaces based on the locations of the previous terminal state and the target waypoint, and then adds some threshold space around them. Samples are drawn from the new space, the query is solved, and then the entire motion plan is followed to the waypoint goal region. Then the process is repeated for the next waypoint in the sequence. By shrinking subsequent goal radii and pre-specifying reasonable position waypoints, the chaser can converge reliably to the final goal.

Sufficiently close in this context implies that any higher-order terms of the linearized relative dynamics are negligible, *e.g.*, within a few percent of the target orbit mean radius

Results

Results demonstrating the active safety policy for comparison with the nominal trajectory (without active safety constraints) are provided here for the survey maneuver shown in Figure 3(c). We first illustrate in Figure 4 the difference in the two motion planning solutions, taken over identical sample sets and subject to the same constraints (excluding active safety). Because of the additional safety constraints placed on the actively-safe solution, the tree of explored paths shown in (b) are a subset of those in (a). The addition of the safety constraint at first has no effect, where the chaser is far from the target and well outside of the Region of Inevitable Collision (RIC) defined by the elliptical Keep-Out Zone (KOZ). However, the plan deviates noticeably in the positive in-track direction while it moves ahead of the target between waypoints 3 and 4, so as to be sure that it will have safe paths available to escape the RIC in the event of a failure. Observe that all escape CAM's also escape the RIC, always executing circularization burns (indicated by the horizontal lines) radially above or below the KOZ. This is as we expected.

We compare the robustness of the two strategies to failures in Figure 5 by examining the mean success rate as a function of the likelihood of thruster failure. Here, each motion plan is simulated with probabilistic control actuation errors and tested to see whether the chaser can successfully complete its mission or otherwise *safely* execute a CAM without violating any of the planning constraints. The "success rate" is defined here as the mean number of safe motion plan or CAM executions per 50 trials, repeated once for each thruster failure probability. Immediately evident is that the actively safe plan works as designed, showing a distinct improvement in success rate over the safety-unconstrained case. We further note that though the spacecraft cannot easily finish its nominal mission when failures occur, actively-safe maneuvers are always available, even for cases of greater than two failures. This indicates that the CAM policy (for both the trajectory and attitude) works quite robustly for the given scenario.

With regards to computational complexity, simulations were run on 100 samples per motion plan, with five motion plans strung together to form a global solution to the overall problem. The current implementation completes its online calculations (including steering between states, calling CollisionFree and Termination, and, if generating an actively safe trajectory, computing and verifying CAM "turn and burn" attitude trajectories) in near-real-time, on the order of minutes per plan. To make the approach amenable to real-time implementation, we plan to pre-compute attitude-trajectories from failure states (samples) as well as leverage recent developments for FMT* parallel processing. We expect these modifications to reduce computation times to the order of seconds.

CONCLUSIONS

This paper explored the use of positively-invariant sets to provide deterministic safety guarantees for the motion planning of autonomous vehicles with uncertain and unpredictable losses of control authority. In short, we argued that for guaranteeing active safety, it is sufficient to enforce that a state is never entered without a viable escape sequence to a safe invariant set from that state, under all possible failure modes. The approach was illustrated for autonomous spacecraft proximity operations in LEO under impulsively-actuated circular CWH dynamics, for a single chaser spacecraft on approach to a single target subject to strict ellipsoidal Keep-Out Zone requirements. The strategy employed, when subject to unrecoverable thruster stuck-off failures, was to enforce a simple one-burn escape maneuver strategy to circularize the spacecraft orbit about a future state along its coasting arc. It was shown that so long as the orbital radius at the circularization point lay outside of the radial band spanned by the target KOZ, the resultant orbit would be guaranteed safe.

Future examinations will attempt to accommodate thruster stuck-on and mis-allocation failures, localization uncertainty, and extension to small-body proximity operations. We also plan to develop risk-constrained approaches that reduce the degree of conservatism inherent in deterministic safety guarantees.

ACKNOWLEDGMENTS
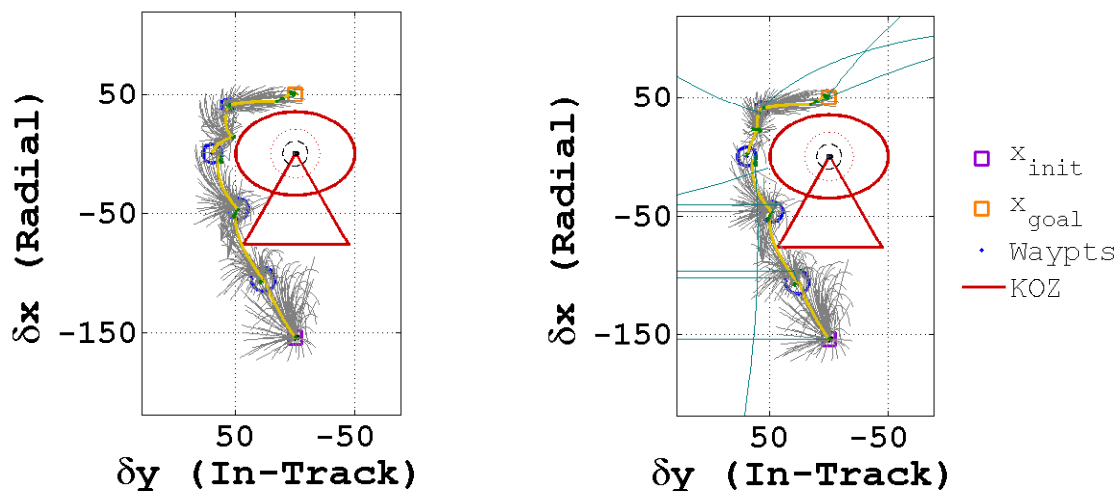
(a) CWH motion plan without active-safety constraints. Under nominal conditions, this is the best path between waypoints amongst the given samples.

(b) CWH motion plan with built-in active safety. Circularization CAMs from each burn location are shown in teal. Along with the nominal path, each is safe (does not pass through the KOZ) and feasible under all two-fault failures.

Figure 4. Comparison between regular and actively-safe motion plans and trees.

APPENDIX A: OPTIMAL CIRCULARIZATION UNDER IMPULSIVE CWH DYNAMICS

The optimization we want to solve, such that we satisfy Definition 3, can be expressed as:

Given: $\quad \mathbf{x}(t), \mathbf{u}(t \leq \tau < T) = \mathbf{0}, \mathbf{u}(T) = \boldsymbol{\Delta}\mathbf{v}_{\text{circ}}(\mathbf{x}(T))$

$\underset{T}{\text{minimize}} \quad \Delta v_{\text{circ}}^2(T)$

subject to $\quad \dot{\mathbf{x}}(\tau) = f(\mathbf{x}(\tau), \mathbf{0}, \tau), t \leq \tau \leq T \qquad$ (Dynamics)

$\qquad\qquad \mathbf{x}(\tau) \notin \mathcal{X}_{\text{KOZ}}, t \leq \tau \leq T \qquad\qquad$ (KOZ Collision Avoidance)

$\qquad\qquad \mathbf{x}(T^+) \in \mathcal{X}_{\text{invariant}} \qquad\qquad\qquad$ (Invariant Set Termination)

Due to the analytical descriptions of state transitions as given in Equation (2), it is a straightforward task to express the decision variable T, invariant set constraint, and objective function analytically in terms of $\theta(t) = n(t - t_0)$, the polar angle of the target spacecraft. The problem is therefore one-dimensional in terms of θ. We can reduce the invariant set termination constraint to an invariant set positioning constraint if we ensure the spacecraft ends up at a position inside $\mathcal{X}_{\text{invariant}}$ and circularize the orbit, since $\mathbf{x}(\theta_{\text{circ}}^+) = \mathbf{x}(\theta_{\text{circ}}^-) + \begin{bmatrix} \mathbf{0} \\ \boldsymbol{\Delta}\mathbf{v}_{\text{circ}}(\theta_{\text{circ}}) \end{bmatrix} \in \mathcal{X}_{\text{invariant}}$. Denote $\theta_{\text{circ}} = n(T - t_0)$ as the target anomaly at which we enforce circularization. Now, suppose the failure state $\mathbf{x}(t)$ satisfies the collision avoidance constraint with the KOZ (otherwise the CAM is infeasible and we conclude $\mathbf{x}$ is unsafe). We can set $\theta_{\text{min}} = n(t - t_0)$ and integrate the coasting dynamics forward until the chaser touches the boundary of the KOZ ($\theta_{\text{max}} = \theta_{\text{collision}}^-$) or for one full orbit ($\theta_{\text{max}} = \theta_{\text{min}} + 2\pi$) such that, between these two bounds, the CAM trajectory satisfies the dynamics and contains only the coasting segment outside of the KOZ. Replacing the dynamics and collision avoidance constraints with the bounds on θ as a box constraint, the problem now reduces to:

$\underset{\theta_{\text{circ}}}{\text{minimize}} \quad \Delta v_{\text{circ}}^2(\theta_{\text{circ}})$

subject to $\quad \theta_{\text{min}} \leq \theta_{\text{circ}} \leq \theta_{\text{max}} \quad$ (Theta Bounds)

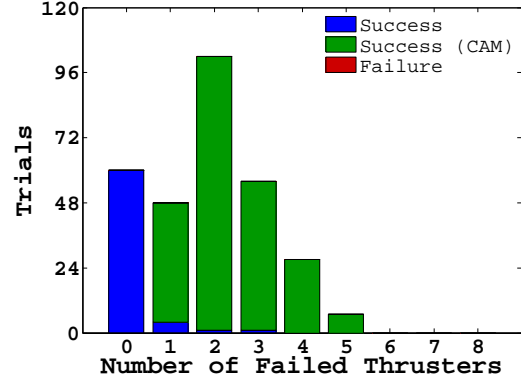$\qquad\qquad \delta x^2(\theta_{\text{circ}}^-) \geq \rho_{\delta x}^2 \qquad$ (Invariant Set Positioning)

Restricting our search range to $\theta \in [\theta_{\text{min}}, \theta_{\text{max}}]$, this is a function of one variable and one constraint,
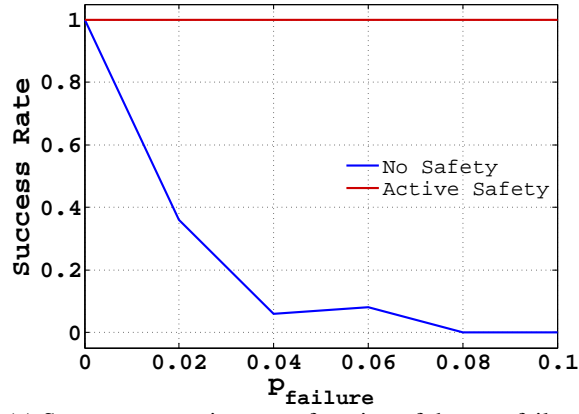
(a) Success comparison as a function of thruster failure probability, computed from 50 trials for each data point.
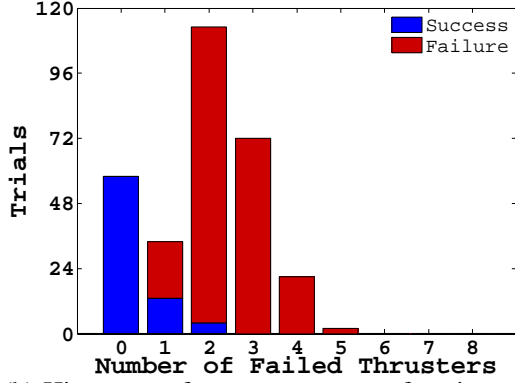
(b) Histogram of success rates as a function of the number of thruster failures for the nominal strategy under failures.

(c) Histogram of success rates as a function of the number of thruster failures for the safety strategy with CAMs.

Figure 5. Measuring the robustness of the CWH active-safety targeting strategy.

something we can easily optimize analytically using the method of Lagrange multipliers. We seek to minimize the Lagrangian, $\mathcal{L} = \Delta v_{\text{circ}}^2 + \lambda g_{\text{circ}}$, where $g_{\text{circ}}(\theta) = \rho_{\delta x}^2 - \delta x^2\left(\theta_{\text{circ}}^-\right)$. There are two cases to consider:

Case 1: Inactive Invariant Set Positioning Constraint   We set $\lambda = 0$ such that $\mathcal{L} = \Delta v_{\text{circ}}^2$. Candidate optimizers θ^* must satisfy $\nabla_\theta \mathcal{L}(\theta^*) = 0$. Taking the gradient of $\mathcal{L}$ and setting $\nabla_\theta \mathcal{L}(\theta^*) = 0$, we find that:

$$\tan 2\theta^* = \frac{-\left(\frac{3}{2}\delta\dot{x}_0(3n\delta x_0 + 2\delta\dot{y}_0) - 2n\delta\dot{z}_0\delta z\right)}{\frac{3}{4}(3n\delta x_0 + 2\delta\dot{y}_0)^2 - \frac{3}{4}\delta\dot{x}_0^2 + n^2\delta z^2 - \delta\dot{z}_0^2}$$

In the general case, this does not admit an analytical solution (its roots must be found numerically). However, it can be shown that for particular conditions on the initial state, the true anomalies (times) θ^* that solve the expression *can* be derived analytically. For instance, for planar maneuvers ($\delta z_0 = \delta\dot{z}_0 = 0$), it can be shown that θ^* occurs where the chaser satisfies $\delta\dot{x}(\theta^*) = 0$ (*i.e.*, at apoapse or periapse, as we might expect). Details are omitted here for brevity. Denote the set of candidate solutions that satisfy Case 1 by Θ_1^*.

Case 2: Active Invariant Set Positioning Constraint   In this case, the chaser spacecraft attempts to circularize its orbit at the boundary of the zero-thrust RIC shown in Figure 2 . The positioning constraint is active,

and therefore $g_{\text{circ}}(\theta) = \rho_{\delta x}^2 - \delta x^2(\theta_{\text{circ}}^-) = 0$. This is equivalent to finding where the coasting trajectory from $\mathbf{x}(t)$ crosses $\delta x(\theta) = \pm\rho_{\delta x}$ for $\theta \in [\theta_{\min}, \theta_{\max}]$. This can be achieved using standard root-finding algorithms. Denote the set of candidate solutions that satisfy Case 2 by Θ_2^*.

Solution to the Minimal-Cost Circularization Burn   The global optimizer θ^* either lies on the boundary of the box constraint, at one of the unconstrained candidate solutions ($\theta \in \Theta_1^*$) or at the boundary of the zero-thrust RIC ($\theta \in \Theta_2^*$), all of which were fortunately economically obtained through either numerical integration or root-finding techniques. Therefore, the minimum-cost circularization burn time T satisfies:

$$\theta^* = n(T - t_0) = \underset{\theta \in \{\theta_{\min}, \theta_{\max}\} \cup \Theta_1^* \cup \Theta_2^*}{\arg\min} \Delta v_{\text{circ}}^2(\theta) \tag{6}$$

If no such solution exists (*e.g.*, if and only if $\mathbf{x}(t)$ starts in the target KOZ), the circularization CAM is declared unsafe. Otherwise, the CAM is saved for feasibility verification.

APPENDIX B: THE STEERING PROBLEM

It is well known that the classical Clohessy-Wiltshire-Hill (CWH) equations [17, 23] for motion about a circular reference orbit are given by a *time-invariant* linear system of form $\dot{\mathbf{x}} = \mathbf{A}\mathbf{x} + \mathbf{B}\mathbf{u}$, where the dynamics matrix $\mathbf{A}$ is a function only of n_{ref} of the client spacecraft orbit, and the input matrix is $\mathbf{B} = [\mathbf{0}_{3\times 3}, \mathbf{I}_{3\times 3}]^{\text{T}}$. The state $\mathbf{x} = [\delta x, \delta y, \delta z, \delta\dot{x}, \delta\dot{y}, \delta\dot{z}]^{\text{T}}$ and the applied force-per-unit-mass $\mathbf{u} = \frac{1}{m}[F_x, F_y, F_z]^{\text{T}}$ of the spacecraft are defined relative to the cross-track, in-track, and out-of-plane directions, respectively, of the client's rotating Local Vertical, Local Horizontal frame. Define $\Phi(t, \tau) \triangleq e^{\mathbf{A}(t-\tau)}$ as the *state transition matrix*. Consider the case of applying N impulsive velocity changes at times $t_0 \le \tau_i \le t_{\text{f}}, i \in [1, \dots, N]$. It can be shown that:

$$\mathbf{x}(t) = \Phi(t, t_0)\mathbf{x}(t_0) + \underbrace{\left[\, \Phi(t,\tau_1)\mathbf{B} \,\middle|\, \dots \,\middle|\, \Phi(t,\tau_N)\mathbf{B} \,\right]}_{\triangleq \mathbf{\Phi}_v(t,\tau_i)} \underbrace{\begin{bmatrix} \mathbf{\Delta v}_1 \\ \vdots \\ \mathbf{\Delta v}_N \end{bmatrix}}_{\triangleq \mathbf{\Delta V}} = \Phi(t,t_0)\mathbf{x}(t_0) + \mathbf{\Phi}_v(t,\tau_i)\mathbf{\Delta V}$$

We can now solve the 2PBVP or "steering problem" between an initial state $\mathbf{x}(t_0) = \mathbf{x}_0$ and final state $\mathbf{x}(t_{\text{f}}) = \mathbf{x}_{\text{f}}$ under CWH dynamics. Substituting and rearranging, we seek a stacked burn vector $\mathbf{\Delta V}$ such that:

$$\mathbf{\Phi}_v(t_{\text{f}}, \tau_i)\mathbf{\Delta V} = \mathbf{x}_{\text{f}} - \Phi(t_{\text{f}}, t_0)\mathbf{x}_0$$

If $N = 2$ (so that $\mathbf{\Phi}_v$ is square) and if it is *non-singular* (that is, the time differences $t_{\text{f}} - \tau_i$ satisfy certain conditions), the solution for $\mathbf{\Delta V}$ is unique and therefore we can use matrix inversion to obtain the solution. If $N \ge 2$, an infinite number of solutions exist. A reasonable choice in this case that minimizes the 2-norm of $\mathbf{\Delta V}$ is the Moore-Penrose pseudo-inverse. Hence, we use:

$$\mathbf{\Delta V} = \begin{cases} \mathbf{\Phi}_v^{-1}(\mathbf{x}_{\text{f}} - \Phi(t_{\text{f}}, t_0)\mathbf{x}_0) & N = 2 \\ \mathbf{\Phi}_v^{\text{T}}\left(\mathbf{\Phi}_v \mathbf{\Phi}_v^{\text{T}}\right)^{-1}(\mathbf{x}_{\text{f}} - \Phi(t_{\text{f}}, t_0)\mathbf{x}_0) & N > 2 \end{cases}$$

to derive *feasible* connections between $\mathbf{x}_0$ and $\mathbf{x}_{\text{f}}$ with N impulses applied at fixed times τ_i. Given N, $\mathbf{x}_0$, $\mathbf{x}_{\text{f}}$, burn magnitude bounds $\Delta v_{\min}, \Delta v_{\max}$ and maneuver duration bounds $d_{\min}, d_{\max}$, we can obtain an *optimal* connection (that minimizes fuel, subject to the given parameters) by solving the *convex* problem:

$$\begin{aligned} \underset{\mathbf{\Delta v}_i, \tau_i, t_{\text{f}}}{\text{minimize}} \quad & \sum_{i=1}^{N} ||\mathbf{\Delta v}_i||_2 \\ \text{subject to} \quad & d_{\min} \le t_{\text{f}} - t_0 \le d_{\max} \\ & t_0 \le \tau_i \le t_{\text{f}} && \text{for all } i \in [1, \dots, N] \\ & \Delta v_{\min} \le ||\mathbf{\Delta v}_i||_2 \le \Delta v_{\max} && \text{for all } i \in [1, \dots, N] \\ & \mathbf{\Phi}_v(t_{\text{f}}, \tau_i)\mathbf{\Delta V} = \mathbf{x}_{\text{f}} - \Phi(t_{\text{f}}, t_0)\mathbf{x}_0 \end{aligned}$$

We solve this for FMT* steering assuming $N = 2$, $\Delta v_{\min} = 0$, $\Delta v_{\max} = \infty$, $d_{\min} = 0$, and $d_{\max} = 0.05\frac{2\pi}{n}$.

REFERENCES

[1] G. Dettleff, "Plume Flow and Plume Impingement in Space Technology," *Progress in Aerospace Sciences*, Vol. 28, No. 1, 1991, pp. 1–71, 10.1016/0376-0421(91)90008-R.

[2] I. D. Boyd and A. Ketsdever, "Interactions Between Spacecraft and Thruster Plumes," *AIAA Journal of Spacecraft and Rockets*, Vol. 38, May 2001, pp. 380–380, 10.2514/2.3712.

[3] W. Fehse, *Automated Rendezvous and Docking of Spacecraft*, Vol. 16. Cambridge University Press, 2003.

[4] M. Haught and G. Duncan, "Modeling Common Cause Failures of Thrusters on ISS Visiting Vehicles," tech. rep., NASA, Jan. 2014. Available at `http://ntrs.nasa.gov/search.jsp?R=20140004797`.

[5] S. M. LaValle and J. J. Kuffner, "Randomized Kinodynamic Planning," *International Journal of Robotics Research*, Vol. 20, No. 5, 2001, pp. 378–400.

[6] J. M. Phillips, L. E. Kavraki, and N. Bedrossian, "Spacecraft Rendezvous and Docking with Real-Time, Randomized Optimization," *AIAA Conf. on Guidance, Navigation and Control*, Austin, TX, Aug. 2003, pp. 1–11.

[7] E. Frazzoli, "Quasi-Random Algorithms for Real-Time Spacecraft Motion Planning and Coordination," *Acta Astronautica*, Vol. 53, Aug. 2003, pp. 485–495.

[8] T. Schouwenaars, J. P. How, and E. Feron, "Receding Horizon Path Planning with Implicit Safety Guarantees," *American Control Conference*, Vol. 6, Boston, MA, June 2004, pp. 5576–5581.

[9] B. J. Naasz, "Safety Ellipse Motion with Coarse Sun Angle Optimization," *Proc. of the NASA GSFC Flight Mechanics Symposium*, Greenbelt, MD, Oct. 2005, pp. 1–13.

[10] D. E. Gaylor and B. W. Barbee, "Algorithms for Safe Spacecraft Proximity Operations," *AAS Meeting*, Vol. 127 of *Advances in the Astronautical Sciences*, Seattle, WA, Jan. 2007, pp. 1–20.

[11] L. Breger and J. P. How, "Safe Trajectories for Autonomous Rendezvous of Spacecraft," *AIAA Journal of Guidance, Control, and Dynamics*, Vol. 31, No. 5, 2008, pp. 1478–1489.

[12] A. Weiss, M. Baldwin, C. Petersen, R. S. Erwin, and I. V. Kolmanovsky, "Spacecraft Constrained Maneuver Planning for Moving Debris Avoidance Using Positively Invariant Constraint Admissible Sets," *American Control Conference*, Washington, DC, June 2013, pp. 4802–4807.

[13] B. W. Barbee, J. R. Carpenter, S. Heatwole, F. L. Markley, M. Moreau, B. J. Naasz, and J. Van Eepoel, "A Guidance and Navigation Strategy for Rendezvous and Proximity Operations with a Noncooperative Spacecraft in Geosynchronous Orbit," *AIAA Journal of the Aerospace Sciences*, Vol. 58, July 2011, pp. 389–408.

[14] T. Schouwenaars, J. P. How, and E. Feron, "Decentralized Cooperative Trajectory Planning of Multiple Aircraft with Hard Safety Guarantees," *AIAA Conf. on Guidance, Navigation and Control*, Providence, RI, Aug. 2004, pp. 1–14, 10.2514/6.2004-5141.

[15] T. Fraichard, "A Short Paper about Motion Safety," *Proc. IEEE Conf. on Robotics and Automation*, Roma, Italy, Apr. 2007, pp. 1140–1145.

[16] J. P. LaSalle, "Some Extensions of Liapunov's Second Method," *IRE Transactions on Circuit Theory*, Vol. 7, Dec. 1960, pp. 520–527, 10.1109/TCT.1960.1086720.

[17] W. H. Clohessy and R. S. Wiltshire, "Terminal Guidance System for Satellite Rendezvous," *AIAA Journal of the Aerospace Sciences*, Vol. 27, Sept. 1960, pp. 653–658.

[18] M. Bodson, "Evaluation of Optimization Methods for Control Allocation," *AIAA Journal of Guidance, Control, and Dynamics*, Vol. 25, July 2002, pp. 703–711.

[19] M. Sharir, "Algorithmic Motion Planning," *Handbook of Discrete and Computational Geometry* (J. E. Goodman and J. O'Rourke, eds.), ch. 40, pp. 733–754, CRC Press, 1997.

[20] S. Karaman and E. Frazzoli, "Sampling-based algorithms for optimal motion planning," *International Journal of Robotics Research*, Vol. 30, No. 7, 2011, pp. 846–894.

[21] L. Janson and M. Pavone, "Fast Marching Trees: A Fast Marching Sampling-Based Method for Optimal Motion Planning in Many Dimensions," *International Symposium on Robotics Research*, 2013.

[22] S. N. Goward, J. G. Masek, D. L. Williams, J. R. Irons, and R. J. Thompson, "The Landsat 7 Mission: Terrestrial Research and Applications for the 21st Century," *Remote Sensing of Environment*, Vol. 78, No. 1–2, 2001, pp. 3–12, 10.1016/S0034-4257(01)00262-0.

[23] G. W. Hill, "Researches in the Lunar Theory," *JSTOR American Journal of Mathematics*, Vol. 1, No. 1, 1878, pp. 5–26.